Nanoscale and Microscale Thermophysical Engineering, 15: 81–94, 2011

ISSN: 1556-7265 print / 1556-7273 online
DOI: 10.1080/15567265.2010.549931

NATURAL CONVECTIVE BOUNDARY LAYER FLOW OVER A NONISOTHERMAL VERTICAL PLATE EMBEDDED IN A POROUS MEDIUM SATURATED WITH A NANOFLUID

Rama Subba Reddy Gorla[1] and Ali Chamkha[2]
[1]*Cleveland State University, Cleveland, Ohio*
[2]*Public Authority for Applied Education and Training, Shuweikh, Kuwait*

Nanofluid refers to a liquid containing a dispersion of submicronic solid particles or nanoparticles. Nanofluids display a thermal conductivity enhancement. This phenomenon suggests the possibility of using nanofluids in electronic cooling and advanced nuclear systems. In this article, a boundary layer analysis is presented for the natural convection past a nonisothermal vertical plate in a porous medium saturated with a nanofluid. Numerical results for friction factor, surface heat transfer rate, and mass transfer rate are presented for parametric variations of the buoyancy ratio parameter, N_r; Brownian motion parameter, N_b; thermophoresis parameter, N_t; Lewis number, Le; and the power law exponent, λ. The dependency of the friction factor, surface heat transfer rate (Nusselt number), and mass transfer rate on these parameters is discussed.

KEY WORDS: natural convection, porous medium, nanofluid

INTRODUCTION

Nanofluids have many applications in industry because materials of nanometer size have unique physical and chemical properties. Nanofluids are solid–liquid composite materials consisting of solid nanoparticles or nanofibers with sizes typically of 1–100 nm suspended in liquid. Nanofluids have attracted great interest recently because of reports of greatly enhanced thermal properties. For example, a small amount ($<1\%$ volume fraction) of Cu nanoparticles or carbon nanotubes dispersed in ethylene glycol or oil is reported to increase the inherently poor thermal conductivity of the liquid by 40 and 150%, respectively [1, 2]. Conventional particle–liquid suspensions require high concentrations ($>10\%$) of particles to achieve such enhancement. However, problems of rheology and stability are amplified at high concentrations, precluding the widespread use of conventional slurries as heat transfer fluids. In some cases, the observed enhancement in thermal conductivity of nanofluids is orders of magnitude greater than that predicted by well-established theories. Other perplexing results in this rapidly evolving field include a surprisingly strong temperature dependence of the thermal conductivity [3] and a threefold higher critical heat flux compared with the base fluids [4, 5]. These enhanced thermal properties are not merely of

Received 22 March 2010; accepted 16 December 2010.
Address correspondence to Rama Subba Reddy Gorla, Cleveland State University, Euclid Avenue at East 24th Street, SH 232, Cleveland, OH 44115. E-mail: r.gorla@csuohio.edu

NOMENCLATURE

D_B	Brownian diffusion coefficient
D_T	thermophoretic diffusion coefficient
f	rescaled nanoparticle volume fraction
g	gravitational acceleration vector
K	permeability of porous medium
k_m	effective thermal conductivity of the porous medium
Le	Lewis number
N_b	Brownian motion parameter
N_r	buoyancy ratio
N_t	thermophoresis parameter
Nu	Nusselt number
P	pressure
q''	wall heat flux
Ra_x	local Rayleigh number
Re	Reynolds number
S	dimensionless stream function
T	temperature
T_W	wall temperature of the vertical plate
T_∞	ambient temperature
U	reference velocity
u, v	Darcy velocity components
(x, y)	Cartesian coordinates

Greek Symbols

α_m	thermal diffusivity of porous medium
β	volumetric expansion coefficient of fluid
ε	porosity
η	dimensionless distance
θ	dimensionless temperature
μ	viscosity of fluid
ρ_f	fluid density
ρ_p	nanoparticle mass density
$(\rho c)_f$	heat capacity of the fluid
$(\rho c)_m$	effective heat capacity of porous medium
$(\rho c)_p$	effective heat capacity of nanoparticle material
τ	parameter defined by Eq. (13)
φ	nanoparticle volume fraction
φ_W	nanoparticle volume fraction at the wall of the vertical plate
φ_∞	ambient nanoparticle volume fraction
ψ	stream function

academic interest. If confirmed and found consistent, they would make nanofluids promising for applications in thermal management. Furthermore, suspensions of metal nanoparticles are being developed for other purposes, such as medical applications including cancer therapy. The interdisciplinary nature of nanofluid research presents a great opportunity for exploration and discovery at the frontiers of nanotechnology.

Porous media heat transfer problems have several engineering applications such as geothermal energy recovery, crude oil extraction, groundwater pollution, thermal energy storage, and flow-through filtering media. Cheng and Minkowycz [6] presented similarity solutions for free convective heat transfer from a vertical plate in a fluid-saturated porous medium. Gorla and Tornabene [7] and Gorla and Zinolabedini [8] solved a nonsimilar problem of free convective heat transfer from a vertical plate embedded in a saturated porous medium with an arbitrarily varying surface temperature or heat flux. The problem of combined convection from vertical plates in porous media was studied by Minkowycz et al. [9] and Ranganathan and Viskanta [10]. All of these studies were concerned with Newtonian fluid flows. The boundary layer flows in nanofluids have been analyzed recently by Nield and Kuznetsov [11, 12]. A clear picture of nanofluid boundary layer flow is still to emerge.

Nanofluids in porous media constitute an emerging topic. Porous foam and microchannel heat sinks used for electronic cooling are optimized utilizing porous media. The utilization of nanofluids for cooling of microchannel heat sinks requires an understanding of the fundamentals of nanofluid convection in porous media.

The present work has been undertaken in order to analyze the natural convection past a nonisothermal vertical plate in a porous medium saturated by a nanofluid. The effects of Brownian motion and thermophoresis are included for the nanofluid. Numerical solutions

of the boundary layer equations are obtained and discussion is provided for several values of the nanofluid parameters governing the problem.

ANALYSIS

We consider the steady free convection boundary layer flow past a vertical plate placed in a nanofluid-saturated porous medium. The coordinate system is selected such that the x-axis is aligned vertically upwards. We consider the two-dimensional problem. We consider a vertical plate at $y = 0$. At this boundary the temperature T and the nanoparticle fraction φ take constant values T_{W} and φ_{W}, respectively. The ambient values, as y tends to infinity, of T and φ are denoted by T_∞ and φ_∞, respectively.

The Oberbeck-Boussinesq approximation is employed and homogeneity and local thermal equilibrium in the porous medium are assumed. We consider the porous medium whose porosity is denoted by ε and permeability by K. The Darcy velocity is denoted by $\vec{v}$. The following four field equations embody the conservation of total mass, momentum, thermal energy, and nanoparticles, respectively. The field variables are the Darcy velocity $\vec{v}$, the temperature T, and the nanoparticle volume fraction φ.

$$\nabla.\vec{\mathrm{v}} = 0 \tag{1}$$

$$\frac{\rho_f}{\varepsilon}\frac{\partial \vec{\mathrm{v}}}{\partial \mathrm{t}} = -\nabla P - \frac{\mu}{K}\mathrm{v} + \left[\phi\rho_{\mathrm{p}} + (1-\phi)\left\{\rho_f\left(1-\beta\left(T-T_\infty\right)\right)\right\}\right]\vec{g} \tag{2}$$

$$(\rho c)_m \frac{\partial T}{\partial t} + (\rho c)_f \vec{\mathrm{v}}\cdot\nabla \mathrm{T} = \mathrm{k_m}\nabla^2 T + \varepsilon\,(\rho c)_p\left[D_B\nabla\phi\cdot\nabla T + \frac{D_T}{T_\infty}\nabla T\cdot\nabla T\right] \tag{3}$$

$$\frac{\partial \phi}{\partial t} + \frac{1}{\varepsilon}\vec{\mathrm{v}}\cdot\nabla\phi = \mathrm{D_B}\nabla^2\phi + \frac{D_T}{T_\infty}\nabla^2 T \tag{4}$$

We write $\vec{v} = (u,v)$.

Here ρ_f, μ, and β are the density, viscosity, and volumetric volume expansion coefficient of the fluid; ρ_{p} is the density of the particles; g is the gravitational acceleration; $(\rho c)_m$ is the effective heat capacity; k_{m} is the effective thermal conductivity of the porous medium; D_{B} is the Brownian diffusion coefficient; and D_{T} is the thermophoretic diffusion coefficient. The flow is assumed to be slow so that an advective term and a Forchheimer quadratic drag term do not appear in the momentum equation.

The boundary conditions are taken as

$$v = 0, \quad T = T_W, \quad \phi = \phi_W, \quad at \quad y = 0, \tag{5}$$

$$u = 0, \quad T \to T_\infty, \quad \phi \to \phi_\infty, \quad as \quad y \to \infty \tag{6}$$

We consider the steady-state flow. In keeping with the Oberbeck-Boussinesq approximation and an assumption that the nanoparticle concentration is dilute, the momentum equation may be written as:

$$0 = -\nabla P - \frac{\mu}{K}\vec{\mathrm{v}} + \left[\left(\rho_P - \rho_{f\infty}\right)\left(\phi-\phi_\infty\right) + \left(1-\phi_\infty\right)\rho_{f\infty}\beta\left(T-T_\infty\right)\right]\vec{g} \tag{7}$$

We now make the standard boundary layer approximation based on a scale analysis and write the governing equations.

$$\frac{\partial u}{\partial x} + \frac{\partial v}{\partial y} = 0 \tag{8}$$

$$\frac{\partial P}{\partial x} = -\frac{\mu}{K}\mathrm{u} + \left[(1-\phi_\infty)\,\rho_{f\infty}\beta g\,(T-T_\infty) - \left(\rho_P - \rho_{f\infty}\right)g\,(\phi-\phi_\infty)\right] \tag{9}$$

$$\frac{\partial P}{\partial y} = 0 \tag{10}$$

$$u\frac{\partial T}{\partial x} + v\frac{\partial T}{\partial y} = \alpha_m \nabla^2 T + \tau\left[D_B\frac{\partial \phi}{\partial y}\frac{\partial T}{\partial y} + \left(\frac{D_T}{T_\infty}\right)\left(\frac{\partial T}{\partial y}\right)^2\right] \tag{11}$$

$$\frac{1}{\varepsilon}\left(u\frac{\partial \phi}{\partial x} + v\frac{\partial \phi}{\partial y}\right) = D_B\frac{\partial^2 \phi}{\partial y^2} + \left(\frac{D_T}{T_\infty}\right)\frac{\partial^2 T}{\partial y^2} \tag{12}$$

where

$$\alpha_m = \frac{k_m}{(\rho c)_f}, \quad \tau = \frac{\varepsilon\,(\rho c)_p}{(\rho c)_f} \tag{13}$$

One can eliminate P from Eqs. (9) and (10) by cross-differentiation. At the same time one can introduce a streamline function ψ such that the continuity is automatically satisfied:

$$u = \frac{\partial \psi}{dy}, \quad v = -\frac{\partial \psi}{dx} \tag{14}$$

We are then left with the following three equations:

$$\frac{\partial^2 \psi}{\partial y^2} = \frac{(1-\phi_\infty)\,\rho_{f\infty}\beta g K}{\mu}\frac{\partial T}{\partial y} - \frac{\left(\rho_P - \rho_{f\infty}\right)gK}{\mu}\frac{\partial \phi}{\partial y} \tag{15}$$

$$\frac{\partial \psi}{\partial y}\frac{\partial T}{\partial x} - \frac{\partial \psi}{\partial x}\frac{\partial T}{\partial y} = \alpha_m \nabla^2 T + \tau\left[D_B\frac{\partial \phi}{\partial y}\frac{\partial T}{\partial y} + \left(\frac{D_T}{T_\infty}\right)\left(\frac{\partial T}{\partial y}\right)^2\right] \tag{16}$$

$$\frac{1}{\varepsilon}\left(\frac{\partial \psi}{\partial y}\frac{\partial \phi}{\partial x} - \frac{\partial \psi}{\partial x}\frac{\partial \phi}{\partial y}\right) = D_B\frac{\partial^2 \phi}{\partial y^2} + \left(\frac{D_T}{T_\infty}\right)\frac{\partial^2 T}{\partial y^2} \tag{17}$$

Proceeding with the analysis, we introduce the following dimensionless variables:

$$\eta = \frac{y}{x}\cdot Ra_x^{1/2}$$

$$Ra_x = \frac{(1-\phi_\infty)\,\rho_{f\infty}\beta g K A x}{\mu\cdot\alpha_m}$$

$$S = \frac{\psi}{\alpha_m\cdot Ra_x^{1/2}}$$

$$\theta = \frac{T-T_\infty}{T_W - T_\infty}$$

$$f = \frac{\phi - \phi_\infty}{\phi_W - \phi_\infty} \tag{18}$$

We assume that

$$T_W - T_\infty = Ax^\lambda$$
$$\phi_W - \phi_\infty = Bx^\lambda$$

where A, B, and λ are constants.

Substituting the expressions in Eq. (18) into the governing Eqs. (15)–(17) we obtain the following transformed equations:

$$S'' - \theta' + N_r \cdot f' = 0 \tag{19}$$

$$\theta'' + \frac{1}{2}S\theta' + N_b \cdot f' \cdot \theta' + N_t \left(\theta'\right)^2 - \lambda.\theta \cdot S' = 0 \tag{20}$$

$$f'' + \frac{1}{2}L_e \cdot S \cdot f' + \frac{N_t}{N_b}\theta'' - \lambda \cdot L_e \cdot S' \cdot f = 0 \tag{21}$$

where the four parameters are defined as:

$$N_r = \frac{\left(\rho_P - \rho_{f\infty}\right)(\phi_W - \phi_\infty)}{\rho_{f\infty}\beta\,(T_W - T_\infty)\,(1 - \phi_\infty)},$$
$$N_b = \frac{\varepsilon\,(\rho c)_P\, D_B\,(\phi_W - \phi_\infty)}{(\rho c)_f\,\alpha_m},$$
$$N_t = \frac{\varepsilon\,(\rho c)_P\, D_T\,(T_W - T_\infty)}{(\rho c)_f\,\alpha_m T_\infty},$$
$$L_e = \frac{\alpha_m}{\varepsilon \cdot D_B}, \tag{22}$$

Here, N_r, N_b, N_t, and Le denote the buoyancy ratio parameter, Brownian motion parameter, thermophoresis parameter, and Lewis number, respectively.

The transformed boundary conditions are as follows:

$$\begin{aligned} \eta = 0: &\quad S = 0, \quad \theta = 1, \quad f = 1 \\ \eta \to \infty: &\quad S' = 0, \quad \theta = 0, \quad f = 0 \end{aligned} \tag{23}$$

The local friction factor may be written as

$$Cf_x = \frac{\left(\mu \frac{\partial u}{\partial y}\right) y = 0}{\frac{\rho U^2}{2}} = \left(2\,[Rax]^{\,T}(3/2).S''(0)\right)/([Rex]^{\,T}2.\,\mathrm{Pr})$$

The heat transfer rate at the surface is given by:

$$q_W = -k_f \left.\frac{\partial T}{\partial y}\right)_{y=0}$$

The heat transfer coefficient is given by:

$$h = \frac{q_W}{(T_W - T_\infty)}$$

The local Nusselt number is given by:

$$Nu_x = \frac{h \cdot x}{k_f} = -Ra_x^{\frac{1}{2}} \cdot \theta'(\xi, 0) \tag{24}$$

The mass transfer rate at the surface is given by:

$$N_W = -D \left.\frac{\partial \phi}{\partial y}\right)_{y=0} = h_m (\phi_W - \phi_\infty)$$

where h_m is the mass transfer coefficient.

The local Sherwood number is given by:

$$Sh = \frac{h_m \cdot x}{D} = -Ra_x^{\frac{1}{2}} \cdot f'(\xi, 0) \tag{25}$$

NUMERICAL METHOD

The system of Eqs. (19)–(21) with the boundary conditions (23) is solved numerically by means of an efficient, iterative, tridiagonal implicit finite-difference method discussed previously by Blottner [13]. Equations (19)–(21) are discretized using three-point central difference formulae with S' replaced by another variable V. The η direction is divided into 196 nodal points and a variable step size is used to account for the sharp changes in the variables in the region close to the surface where viscous effects dominate. The initial step size used is $\Delta\eta_1 = 0.001$ and the growth factor $K = 1.037$ such that $\Delta\eta_n = K\Delta\eta_{n-1}$ (where the subscript n is the number of nodes minus one). This gives $\eta_{\max} \approx 35$, which represents the edge of the boundary layer at infinity. The ordinary differential equations are then converted into linear algebraic equations that are solved by the Thomas algorithm discussed by Blottner [13]. Iteration is employed to deal with the nonlinear nature of the governing equations. The convergence criterion employed in this work was based on the relative difference between the current and the previous iterations. When this difference or error reached 10^{-5}, the solution was assumed to be converged and the iteration process was terminated.

RESULTS AND DISCUSSION

Equations (19)–(21) were solved numerically to satisfy the boundary conditions (23) for parametric values of Le, N_r, N_b, N_t, and power law exponent λ using a finite difference method. Tables 1–5 indicate results for wall values for the gradients of velocity, temperature, and concentration functions, which are proportional to the friction factor, Nusselt number, and Sherwood number, respectively. From Tables 1–3, we notice that as N_r and N_t increase, the friction factor increases, whereas the heat transfer rate (Nusselt number) and mass transfer rate (Sherwood number) decrease. As N_b increases, the friction factor and surface mass transfer rates increase, whereas the surface heat transfer rate decreases.

Table 1 Effects of N_r on $S''(0)$, $-\theta'(0)$, and $-f'(0)$ for $N_b = 0.3$, $N_t = 0.1$, $Le = 10$, and $\lambda = 0$

N_r	$S''(0)$	$-\theta'(0)$	$-f'(0)$
0.1	−0.0180685	0.3297846	1.619866
0.2	−0.0010914	0.3227547	1.556346
0.3	0.0145055	0.3149958	1.489373
0.4	0.0283915	0.3072273	1.419391
0.5	0.0408457	0.2980915	1.344729

Table 2 Effects of N_t on $S''(0)$, $-\theta'(0)$, and $-f'(0)$ for $N_b = 0.3$, $N_r = 0.5$, $Le = 10$, and $\lambda = 0$

N_t	$S''(0)$	$-\theta'(0)$	$-f'(0)$
0.1	0.0408457	0.2980915	1.344729
0.2	0.0418536	0.2855166	1.337651
0.3	0.0428675	0.2740883	1.334341
0.4	0.0440512	0.2628078	1.334338
0.5	0.0454118	0.2522424	1.337451

Table 3 Effects of N_b on $S''(0)$, $-\theta'(0)$, and $-f'(0)$ for $N_r = 0.5$, $N_t = 0.1$, $Le = 10$, and $\lambda = 0$

N_b	$S''(0)$	$-\theta'(0)$	$-f'(0)$
0.1	0.0312239	0.3437461	1.260950
0.2	0.0371269	0.3210715	1.321422
0.3	0.0408457	0.2980915	1.344729
0.4	0.0439665	0.2761186	1.359024
0.5	0.0468399	0.2547152	1.369532

Table 4 Effects of Le on $S''(0)$, $-\theta'(0)$, and $-f'(0)$ for $N_b = 0.3$, $N_r = 0.5$, $N_t = 0.1$, and $\lambda = 0$

Le	$S''(0)$	$-\theta'(0)$	$-f'(0)$
1	−0.0143592	0.2627161	0.2599934
10	0.0408457	0.2980915	1.344729
100	0.2143756	0.3091981	4.557745
1,000	0.7621598	0.3139326	14.63052

Table 5 Effects of λ on $S''(0)$, $-\theta'(0)$, and $-f'(0)$ for $N_b = 0.3$, $N_r = 0.5$, $N_t = 0.1$, and $Le = 10$

λ	$S''(0)$	$-\theta'(0)$	$-f'(0)$
0	0.0408457	0.2980915	1.344729
0.5	0.0600894	0.4905557	2.080914
1.0	0.0748478	0.6338331	2.636901

Results from Table 4 indicate that as *Le* increases, the heat and mass transfer rates increase. From Table 5, we observe that as λ increases, the heat and mass transfer rates increase. Therefore, our current results indicate that nonisothermal surfaces promote higher heat and mass transfer rates in nanofluid boundary layers.

Figures 1–3 indicate that as N_r increases, the velocity decreases and the temperature and concentration increase. Similar effects are observed from Figures 4–9 as N_t and N_b vary.

Figures 10 illustrates the variation of velocity within the boundary layer as *Le* increases. The velocity increases as *Le* increases. From Figures 11 and 12, we observe that as *Le* increases, the temperature and concentration within the boundary layer decrease and the thermal and concentration boundary later thicknesses decrease. Figures 13–15 indicate that as the power law exponent λ increases, the velocity increases, whereas the temperature and concentration within the boundary layer decrease.

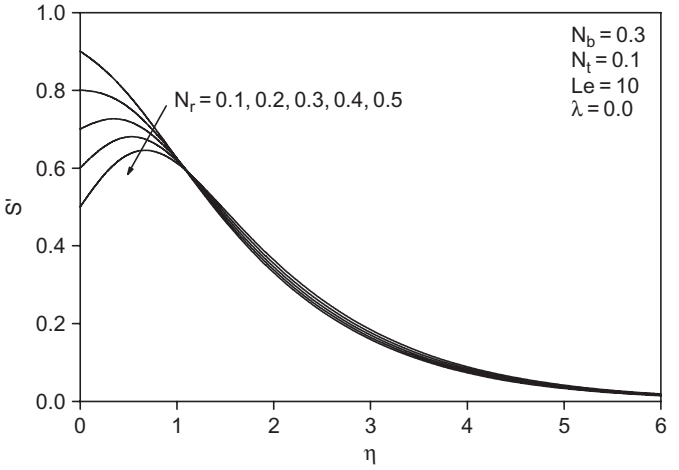

Figure 1 Effects of N_r on velocity profiles.

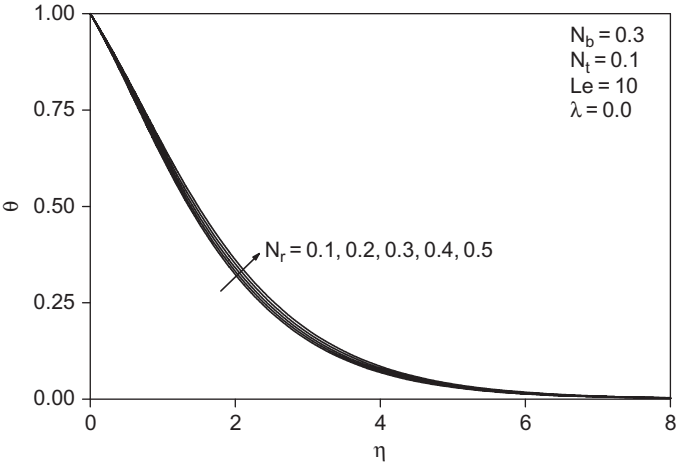

Figure 2 Effects of N_r on temperature profiles.

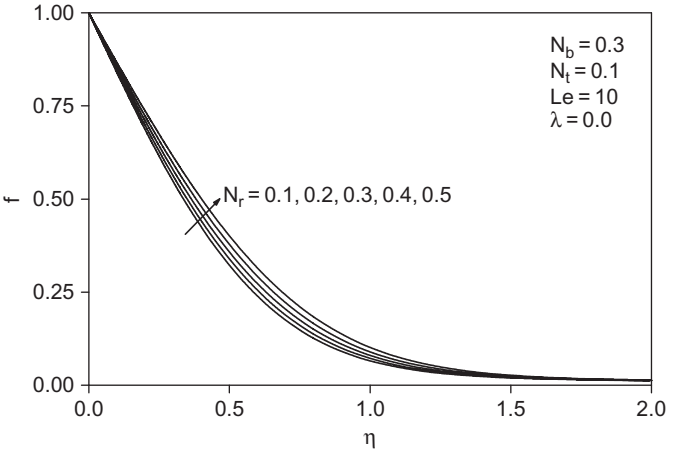

Figure 3 Effects of N_r on volume fraction profiles.

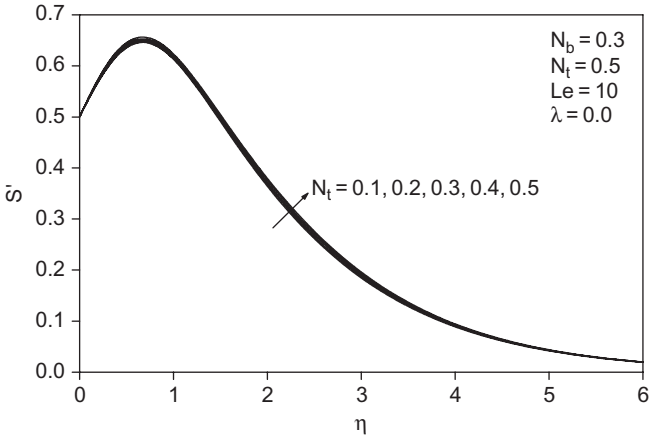

Figure 4 Effects of N_t on velocity profiles.

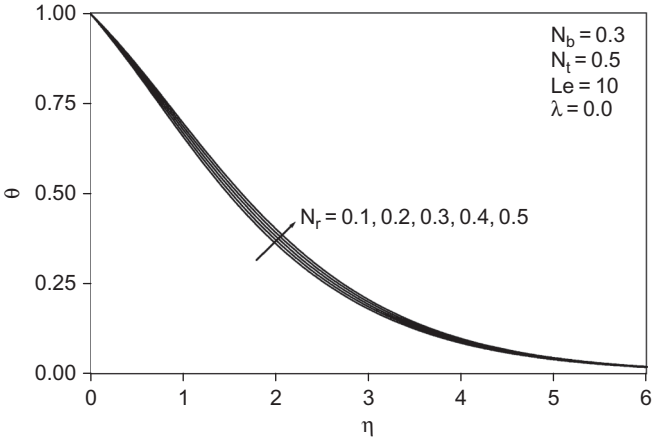

Figure 5 Effects of N_t on temperature profiles.

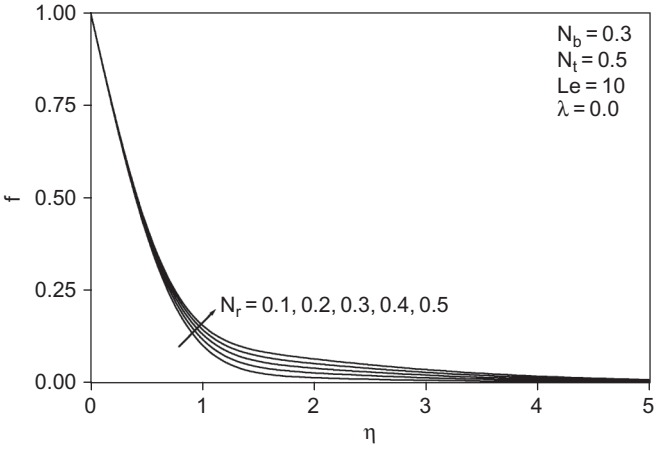

Figure 6 Effects of N_t on volume fraction profiles.

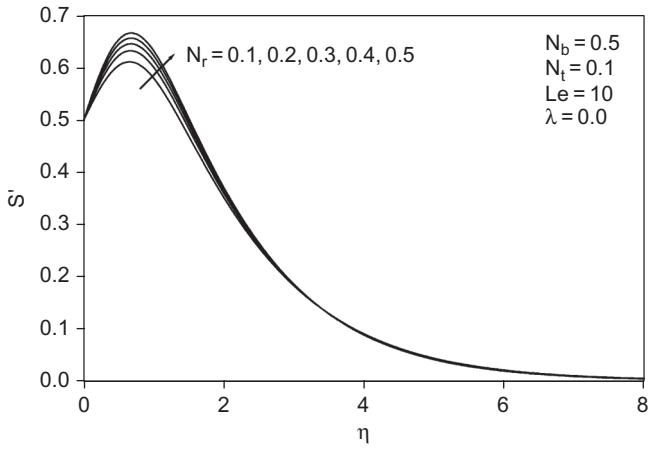

Figure 7 Effects of N_b on velocity profiles.

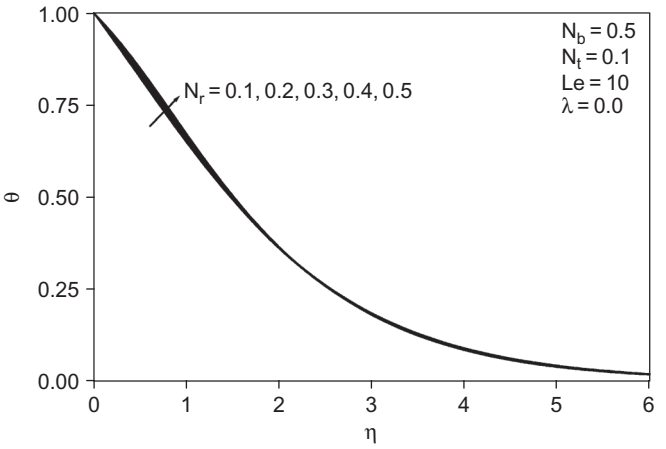

Figure 8 Effects of N_b on temperature profiles.

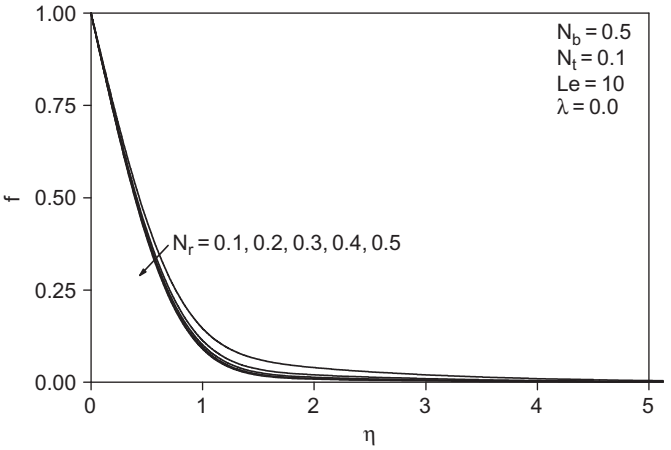

Figure 9 Effects of N_b on volume fraction profiles.

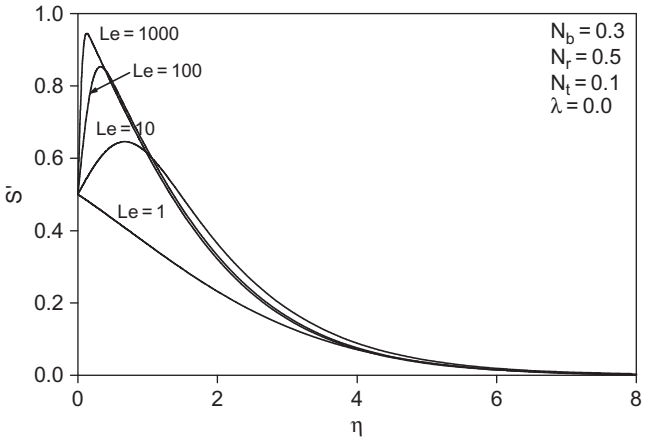

Figure 10 Effects of *Le* on velocity profiles.

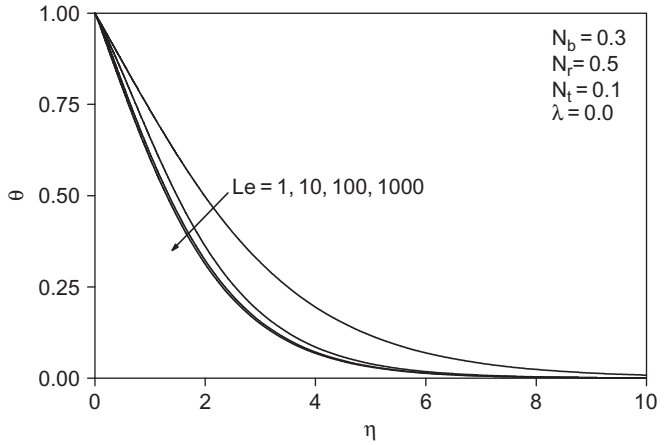

Figure 11 Effects of *Le* on temperature profiles.

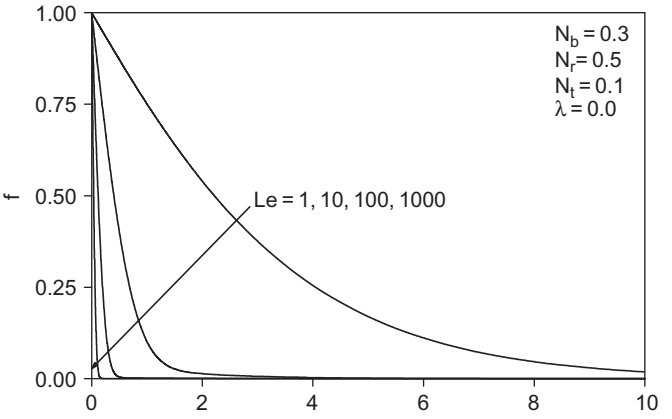

Figure 12 Effects of *Le* on volume fraction profiles.

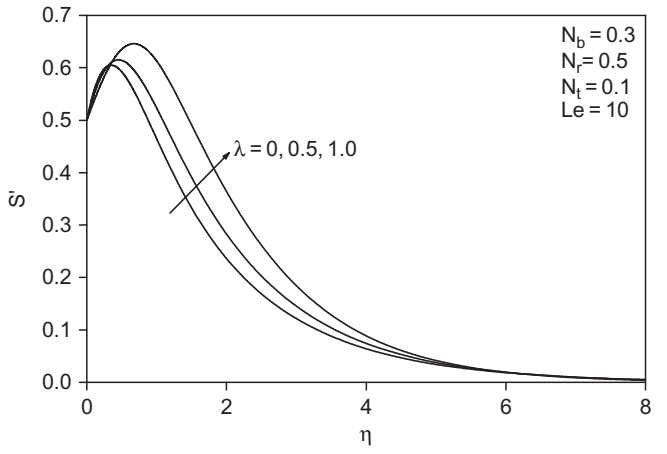

Figure 13 Effects of λ on velocity profiles.

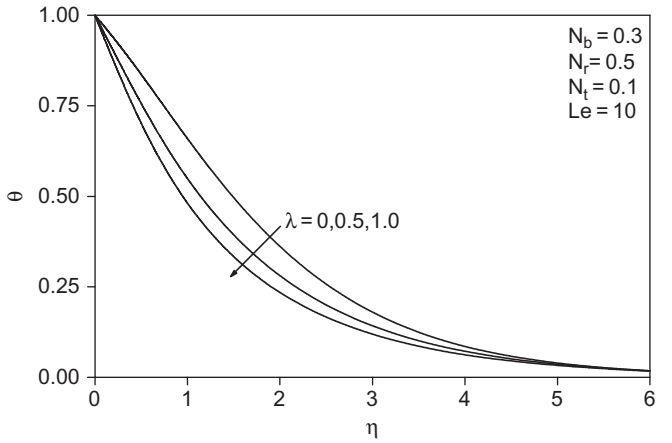

Figure 14 Effects of λ on temperature profiles.

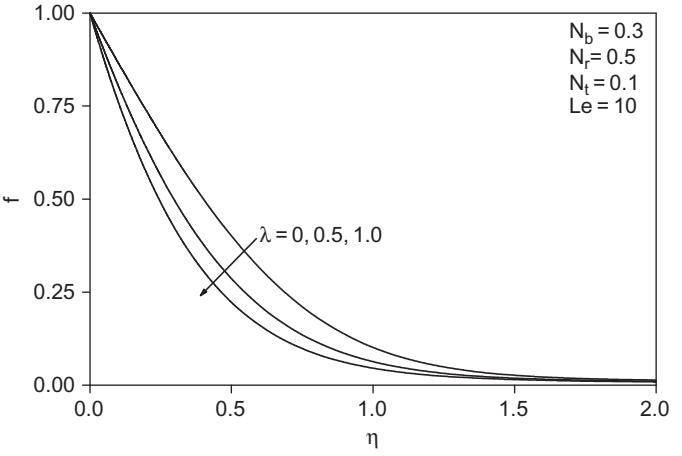

Figure 15 Effects of λ on volume fraction profiles.

The influence of nanoparticles on natural convection is modeled by accounting for Brownian motion and thermophoresis as well as nonisothermal boundary conditions. The thickness of the boundary layer for the mass fraction is smaller than the thermal boundary layer thickness for large values of *Le*. The contribution of N_t to heat and mass transfer does not depend on the value of *Le*. The Brownian motion and thermophoresis of nanoparticles increase the effective thermal conductivity of the nanofluid. Both Brownian diffusion and thermophoresis give rise to cross-diffusion terms that are similar to the familiar Soret and Dufour cross-diffusion terms that arise with a binary fluid discussed by Lakshmi Narayana et al. [14].

CONCLUDING REMARKS

In this article, we presented a boundary layer analysis for the natural convection past a nonisothermal vertical plate in a porous medium saturated with a nanofluid. Numerical results for friction factor, surface heat transfer rate, and mass transfer rate are presented for parametric variations of the buoyancy ratio parameter N_r, Brownian motion parameter N_b, thermophoresis parameter N_t, and Lewis number *Le*. The results indicate that as N_r and N_t increase, the friction factor increases, whereas the heat transfer rate (Nusselt number) and mass transfer rate (Sherwood number) decrease. As N_b increases, the friction factor and surface mass transfer rates increase, whereas the surface heat transfer rate decreases. As *Le* increases, the heat and mass transfer rates increase. As the power law exponent λ increases, the heat and mass transfer rates increase.

REFERENCES

1. J.A. Eastman, S.U.S. Choi, S. Li, W. Yu, and L.J. Thompson, Anomalously Increased Effective Thermal Conductivities Containing Copper Nanoparticles, *Applied Physics Letters*, vol. 78, pp. 718–720, 2001.
2. S.U.S. Choi, Z.G. Zhang, W. Yu, F.E. Lockwood, and E.A. Grulke, Anomalous Thermal Conductivity Enhancement on Nanotube Suspensions, *Applied Physics Letters*, vol. 79, pp. 2252–2254, 2001.

3. H.E. Patel, S.K. Das, T. Sundararajan, A. Sreekumaran, B. George, and T. Pradeep, Thermal Conductivities of Naked and Monolayer Protected Metal Nanoparticle Based Nanofluids: Manifestation of Anomalous Enhancement and Chemical Effects, *Applied Physics Letters*, vol. 83, pp. 2931–2933, 2003.
4. S.M. You, J.H. Kim, and K.H. Kim, Effect of Nanoparticles on Critical Heat Flux of Water in Pool Boiling Heat Transfer, *Applied Physics Letters*, vol. 83, pp. 3374–3376, 2003.
5. P. Vassallo, R. Kumar, and S. D'Amico, Pool Boiling Heat Transfer Experiments in Silica–Water Nonofluids, *International Journal of Heat and Mass Transfer*, vol. 47, pp. 407–411, 2004.
6. P. Cheng, and W.J. Minkowycz. Free Convection about a Vertical Flat Plate Embedded in a Saturated Porous Medium with Applications to Heat Transfer from a Dike, *Journal of Geophysics Research*, vol. 82, pp. 2040–2044, 1977.
7. R.S.R. Gorla and R. Tornabene, Free Convection from a Vertical Plate with Nonuniform Surface Heat Flux and Embedded in a Porous Medium, *Transport in Porous Media*, vol. 3, pp. 95–106, 1988.
8. R.S.R. Gorla and A. Zinolabedini, Free Convection from a Vertical Plate with Nonuniform Surface Temperature and Embedded in a Porous Medium, Transactions of ASME, *Journal of Energy Resources Technology*, vol. 109, pp. 26–30, 1987.
9. W.J. Minkowycz, P. Cheng, and C.H. Chang, Mixed Convection about a Nonisothermal Cylinder and Sphere in a Porous Medium, *Numerical Heat Transfer*, vol. 8, pp. 349–359, 1985.
10. P. Ranganathan and R. Viskanta, Mixed Convection Boundary Layer Flow along a Vertical Surface in a Porous Medium, *Numerical Heat Transfer*, vol. 7, pp. 305–317, 1984.
11. D.A. Nield and A.V. Kuznetsov, The Cheng-Minkowycz Problem for Natural Convective Boundary Layer Flow in a Porous Medium Saturated by a Nanofluid, *International Journal of Heat and Mass Transfer*, vol. 52, pp. 5792–5795, 2009.
12. D.A. Nield and A.V. Kuznetsov, Thermal Instability in a Porous Medium Layer Saturated by a Nanofluid, *International Journal of Heat and Mass Transfer*, vol. 52, pp. 5796–5801, 2009.
13. F.G. Blottner, Finite-Difference Methods of Solution of the Boundary-Layer Equations, *AIAA Journal*, vol. 8, pp. 193–205, 1970.
14. P.A. Lakshmi Narayana, P.V.S.N. Murthy, and R.S.R. Gorla, Soret-Driven Thermosolutal Convection Induced by Inclined Thermal and Solutal Gradients in a Shallow Horizontal Layer of a Porous Medium, *Journal of Fluid Mechanics*, vol. 612, pp. 1–19, 2008.